Heliyon 10 (2024) e35770

Contents lists available at ScienceDirect

Heliyon

journal homepage: www.cell.com/heliyon

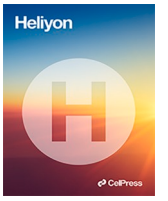

Research article

The microenvironmental factors induced invasive tumor cells in glioblastoma

Jianyu Zhang [a], Jinghui Li [a], Renli Qi [a], Shipeng Li [a], Xin Geng [a], Hong Shi [b,**], Hualin Yu [a,*]

[a] Second Department of Neurosurgery, Kunming Medical University First Affiliated Hospital, Kunming, Yunnan, China
[b] State Key Laboratory of Primate Biomedical Research, Institute of Primate Translational Medicine, Kunming University of Science and Technology, Kunming, Yunnan, China

ARTICLE INFO

Keywords:
Single cell RNA-seq
Intratumoral heterogeneity
Tumor microenvironment
Tumor invasion

ABSTRACT

Glioblastoma (GBM) cells have the potential to switch from being "proliferative cells" to peritumoral "invasive cells". Peritumoral GBM cells have highly invasive properties that allow them to survive surgery, leading to recurrence. The mechanisms underlying the manner in which the tumor microenvironment (TME) regulates the invasiveness of GBM remain unclear. Single-cell RNA sequencing analysis revealed heterogeneity in GBM cells, microglia and macrophages. In this study, the Oncostatin M receptor (OSMR) and leukemia inhibitory factor receptor (LIFR) expression indicated higher invasiveness in core GBM cells. Under environmental stress, the expression of OSMR and LIFR were up-regulated with the effect of hypoxic, acidic, and low-glucose conditions *in vitro*. Functional experiments revealed that TME stress significantly influences the proliferation, migration and invasion of GBM cells. The differences in core/peripheral TMEs in GBM affected the invasive properties, indicating the significant role of OSMR expression within the TME in tumor progression and postoperative therapy.

1. Introduction

Glioblastoma (GBM) is the most common and malignant primary tumor of the central nervous system, with an extremely poor prognosis [1]. It is characterized by an aggressive progression, high recurrence and mortality rates [2]. Pathological studies have suggested that a subset of GBM cells with high migratory and invasive properties infiltrate the peritumoral region during tumor progression. These GBM cells survived from surgery and resulted in recurrence [3]. The "go or grow" mechanism, also known as migration/proliferation dichotomy, is a framework that has allowed for a deeper understanding of the dynamics of "invasive GBM cells". "Go" refers to the invasive and migratory properties, and "grow" refers to the proliferative properties of GBM cells. Evidence has indicated that cell movement and proliferation are mutually exclusive [4]. GBM cells can be divided into two phenotypes: "proliferative" and "invasive". Phenotypic shifts involve a series of biological changes, including extracellular matrix remodeling, cytoskeletal regulation, and mesenchymal trait acquisition [2].

The tumor microenvironment (TME) plays an active role in these phenotypic shifts, particularly in tumor progression [5]. The TME in GBM has been shown to consist of microglia, astrocytes, endothelial cells, the extracellular matrix, and metabolites [6,7]. High

* Corresponding author.
** Corresponding author.
E-mail addresses: shih@kust.edu.cn (H. Shi), yuhl308@126.com (H. Yu).

https://doi.org/10.1016/j.heliyon.2024.e35770
Received 7 April 2024; Received in revised form 7 July 2024; Accepted 2 August 2024
Available online 3 August 2024

energy demand in GBM cells with an inadequate supply of oxygen and nutrients results in hypoxia, low glucose levels, and acidity [8]. TME stresses, such as hypoxia and glucose starvation, have been shown to increase the invasiveness of GBM cells [9] indirectly. However, the mechanism and direct effect of the TME on cell invasiveness need to be verified. The mechanism of the phenotypic shift could hopefully decode the invasive growth of GBM cells.

Bulk RNA sequencing plays an indispensable role, but it mainly focuses on tumor entities without cell level precision [10]. Invasive GBM cells in the peritumoral tissue could not be extracted and analyzed separately until single-cell RNA sequencing (scRNA-seq) analysis was performed. scRNA-seq can reveal gene expression characteristics in an individual cell, making it feasible to capture the molecular features of peritumoral cancer cells [11]. Studies have performed scRNA-seq in patients [12,13]. Statistical and biological differences were observed between the regions but analysis of GBM invasiveness was inadequate.

Appropriate marker genes for GBM invasiveness would help identify GBM subgroups with invasive properties. Oncostatin M (OSM) and leukemia inhibitory factor (LIF) are members of the interleukin-6 (IL-6) family of cytokines [14], which were predominantly secreted by macrophages/microglia. Their receptors, Oncostatin M receptor (OSMR) and leukemia inhibitory factor receptor (LIFR) were the key regulatory factors in GBM development [15,16]. Multiple studies have confirmed that OSMR promote the invasion and migration of GBM cells [17]. LIFR participates in cancer stem cell (CSC) renew and suppression of invasion and metastasis [18]. Overall, the expression of LIFR/OSMR revealed the invasiveness of GBM cells.

In this study, based on scRNA-seq data, the heterogeneity between core and peripheral GBM cells was analyzed, especially genes and pathways that were associated with GBM progression and invasion. The relationship among TME stress, LIFR/OSMR expression, and motility/proliferation of GBM cells was validated *in vitro*.

2. Materials and methods

2.1. Single-cell RNA-Seq data acquisition and processing

Raw data used in this study were obtained from the GEO database (GSE84465, http://www.ncbi.nlm.nih.gov/geo/), which contains 3589 cells from four GBM patients [11]. Among these cells, 2343 cells were collected from the tumor core region and 1246 from the peripheral region, according to the metadata from the GEO database.

Quality control, normalization, and statistical analysis of scRNA-seq data were performed in R 4.1.2, using the Seurat package [19]. Quality control was performed based on the following standards: 1) exclude genes expressed in less than three cells, 2) exclude cells with less than 50 genes detected, and 3) exclude cells with more than 5 % of mitochondrial genes [12]. After data normalization, principal component analysis (PCA) was performed using a linear dimensional reduction method. The t-SNE and UMAP were applied to gather similar cells with low dimensions.

After obtaining the marker genes for each cluster, the R package, scCATCH, was used to identify each cluster [20]. SingleR was used to verify the reliability of cluster identification [21]. Differential expression analysis was performed in the package DESeq2 [22]. Gene set enrichment analysis (GSEA) based on multiple genesets (www.gsea-msigdb.org) was performed using the package GSEABase [23]. The CellChat package was used to perform the intercellular communication analysis [24,25].

2.2. TCGA data analysis

Overall survival and gene expression analyses in different GBM subtypes were performed using the Gene Expression Profiling Interactive Analysis 2 (GEPIA2; gepia2.cancer-pku.cn) using the TCGA database [26].

2.3. Cell culture

The human glioblastoma cell lines U87 (iCell-h224) and U251 (iCell-h219) were obtained from iCell Bioscience Inc. (Shanghai, China). The cells were maintained at 37 °C in a humidified 5 % CO_2 atmosphere and cultured in a complete medium consisting of Dulbecco's modified Eagle's medium (DMEM, Gibco), 10 % fetal bovine serum (FBS, Gibco), and 1 % penicillin-streptomycin (Solarbio).

2.4. Culture conditions to simulate TME

This study used three culture conditions (i.e., glucose deprivation, hypoxia, and acidity). Specifically, the glioma microenvironment representative of each of these conditions was simulated as follow [9,27].

(1) Using low-glucose (1 g/L) DMEM was used to simulate glucose deprivation [27];
(2) $CoCl_2$with final concentration as 150 μM was used in hypoxic condition [28];
(3) To simulate an acidic environment, the complete medium was adjusted to pH 6.5 using PIPES buffer solution and hydrochloric acid [29].

2.5. RNA extraction and real-time PCR

Cells were seeded in six-well plates and cultured in a complete medium for 12 h before stress exposure to maintain minimal

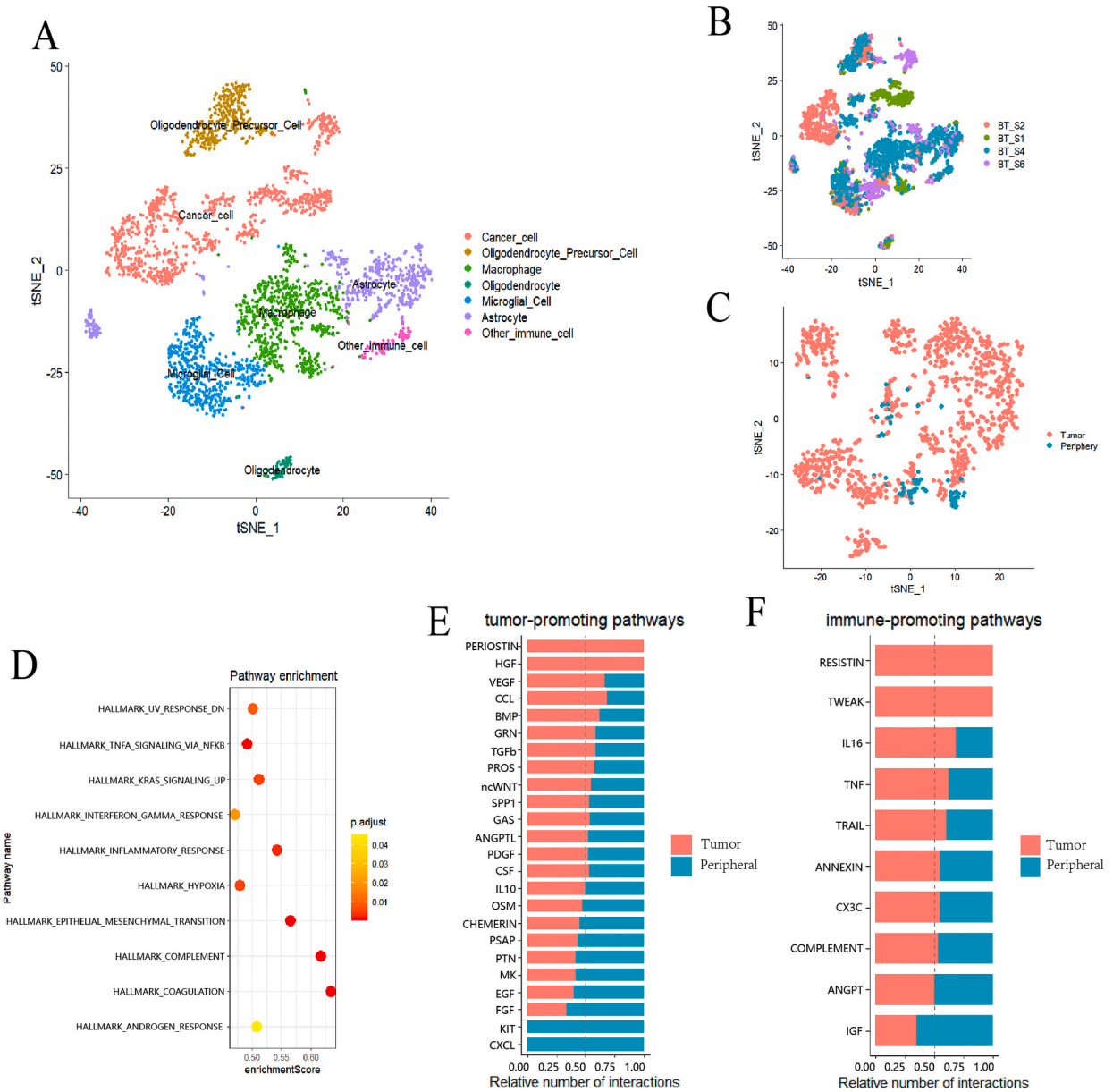

Fig. 1. | ScRNA-seq analysis revealed the heterogeneity of core/peripheral TMEs. **(A)** Different types of cells clustered respectively on the tSNE map. **(B)** Cells from each patient gathered at varying degrees due to the inter-patient heterogeneity. **(C)** Peripheral GBM cells clustered closely. **(D)** Enrichment of differential genes in core/peripheral GBM cells. **(E)** Ranknet plot of tumor-promoting and immune-promoting pathways.

differences in cell viability. The culture medium was replaced with conditioned media after fixing the cells twice with phosphate buffered saline (PBS). After 48 h of exposure to glucose deprivation, hypoxia, or acidity, the total RNA was extracted using an RNA extraction kit (RNAeasy™ Plus Animal RNA Isolation Kit with a Spin Column, Beyotime). RNAs were then subjected to reverse transcription using the BeyoRT™ II First Strand cDNA Synthesis Kit (RNase H minus).

Real-time quantitative polymerase chain reaction (qRT-PCR) was performed using the iTaq Universal SYBR Green Supermix (Bio–Rad). Primers for qRT-PCR were designed using NCBI primer-blast (https://www.ncbi.nlm. nih.gov/tools/primer-blast/).

Hypoxia-inducible factor-1A (HIF1A), a hypoxia sensor gene, was used to verify that the cells sensed hypoxic conditions after the treatment of $CoCl_2$ [30,31]. Acid-sensing ion channel subunit 1 (ASIC1) was chosen as the sensor gene of acidity, which is upregulated when environmental pH = 6.5 [32]. Nuclear factor erythroid 2 like 1 (NFE2L1), which functions as a sensor of the cellular energy state, was used to verify the low-glucose conditions [33]. β-actin (ACTB) was chosen as an internal reference gene to normalize mRNA expression in qRT–PCR [34].

The sequences of primers for qPCR are shown in Supplementary Table S1.

2.6. Cell proliferation assay

For the proliferation assay, the cells were seeded in 96-well Plates at a density of 5000 cells per well. After 12 h of culture to ensure cell adherence, the medium was replaced with a conditioned medium. Considering that the OD value might be disturbed by the color of the medium, control groups were set for each condition. Then, 10 μl of Cell Counting Kit 8 (CCK-8) reagent was added and OD value at 450 nm was recorded at 0, 1.5 and 4 h.

2.7. Wound-healing assay

GBM cells were seeded in 6-well plates at a density of 4.5×10^5 cells per well and incubated to achieve 90 % confluence. Cells were cultured in DMEM supplemented with 1 % FBS for 6h. Wounds were scratched using 200 μl pipette tips. After washing twice with PBS, the cells were cultured in a conditional medium containing 1 % FBS. The wounds were imaged at 0h, and 16 or 24 h, and 12 fields were captured per well. The measurements and healing rate calculations were performed using ImageJ software (https://imagej.net/ij/).

2.8. Transwell invasion assay

The Matrigel invasion chamber was pre-treated for the cell invasion assay according to the manufacturer's instructions. $8\text{-}10 \times 10^4$ cells/well were seeded in the inner chamber with a serum-free conditioned medium, whereas the medium in the outer chamber was consisted of 20 % FBS. After 24 or 30 h of incubation, the cells passing through the PC membrane were fixed with 4 % paraformaldehyde and stained with crystal violet. Nine representative 100X fields per well were used for imaging. The cell numbers were analyzed and counted using the ImageJ software.

2.9. Statistical analysis

All the quantified data were presented as mean ± SD. Statistical differences between two groups were analyzed using Student's t-test. $p < 0.05$. significant.

3. Results

3.1. ScRNA-seq analysis revealed the regional characteristics in GBM

A total of 3589 cells and 19,456 genes were included in the analysis. The t-distributed stochastic neighbor embedding (tSNE) algorithm was applied, and the cells were classified into 13 clusters. Four of these clusters were recognized as GBM cells (labeled as "cancer cells") with 1119 cells. Non-tumor cells were found to host macrophages, astrocytes, microglia, oligodendrocyte precursor cells, oligodendrocytes, and "other immune cells". Different cell types clustered on the tSNE map (Fig. 1A). Cells from each patient were also gathered to varying degrees owing to interpatient heterogeneity (Fig. 1B). After the annotation, all cell types were separately divided into core and peripheral groups based on their regions, for further analysis.

Peripheral GBM cells were closely distributed (Fig. 1C), indicating common regional features. For further investigation of regional features, 4126 differential genes were obtained using the DESeq2 package in core versus peripheral GBM cells (adjusted $p < 0.05$). Among the differentially expressed genes, 3931 were upregulated and 195 were downregulated.

GSEA revealed the biological implications of the differentially expressed genes (Fig. 1D), including epithelial-mesenchymal transition, inflammatory response, and hypoxia. Immune interactions and environmental stress have a strong impact on GBM. We also found other tumor-associated enrichment results, such as EGFR upregulation corresponding to the hypoxic TME, which induced angiogenesis; downregulation of P53 and PTEN indicated the tumorigenesis process inside of the tumor mass.

A comparison of tumor-associated microglia/macrophages (TAMs) (core vs. peripheral) revealed differential expression of marker genes of the M1 or M2 phenotype. Marker genes of M1 phenotype (such as TNF and IL-1β) decreased in the core area, while TGFβ and IL-10, as the marker genes of M2 phenotype, were upregulated ($\log2\text{FoldChange} > |1|$, adjusted $p < 0.05$). The expression of the marker genes showed M2 phenotype-like characteristics of TAMs. These features imply a role for TAMs in anti-inflammatory effects and tumor promotion.

Intercellular communication was analyzed using the CellChat package (Figs. S1A and B). 47 pathways were sorted out and categorized as tumor-promoting, immune-promoting or none. Although there were differences between core/peripheral TMEs, the Ranknet plot presented a balanced state of tumor promotion (Fig. 1E and F). The tumor-promoting pathways (such as TGF-β and CXCL12) exceeded the immune-promoting pathways (such as TNF), which implied the dominating role of GBM cells in intercellular interaction.

Differential expression of OSMR and LIFR in scRNA-seq data and models *in vitro* indicated different invasiveness of core and peripheral GBM cells.

TCGA overall survival analysis showed a negative effect of OSMR on patients' survival while limiting the effect of LIFR (Figs. S2A and B). The mesenchymal GBM subtype showed the highest OSMR expression and slightly different LIFR expression (Figs. S2C and D).

In the scRNA-seq analysis, OSMR was significantly upregulated in core versus peripheral GBM cells ($p < 0.005$), whereas LIFR was decreased ($p < 0.05$). Further, the interaction patterns of "OSM" and "LIFR" in intercellular communication analysis presented obvious differences (Figs. S1C and D). LIF and OSM showed no significant differences between the two groups. This non-differential expression of ligands confirmed that macrophages/microglia play a small role in OSMR/LIFR and GBM invasion-related pathways. Enrichment in

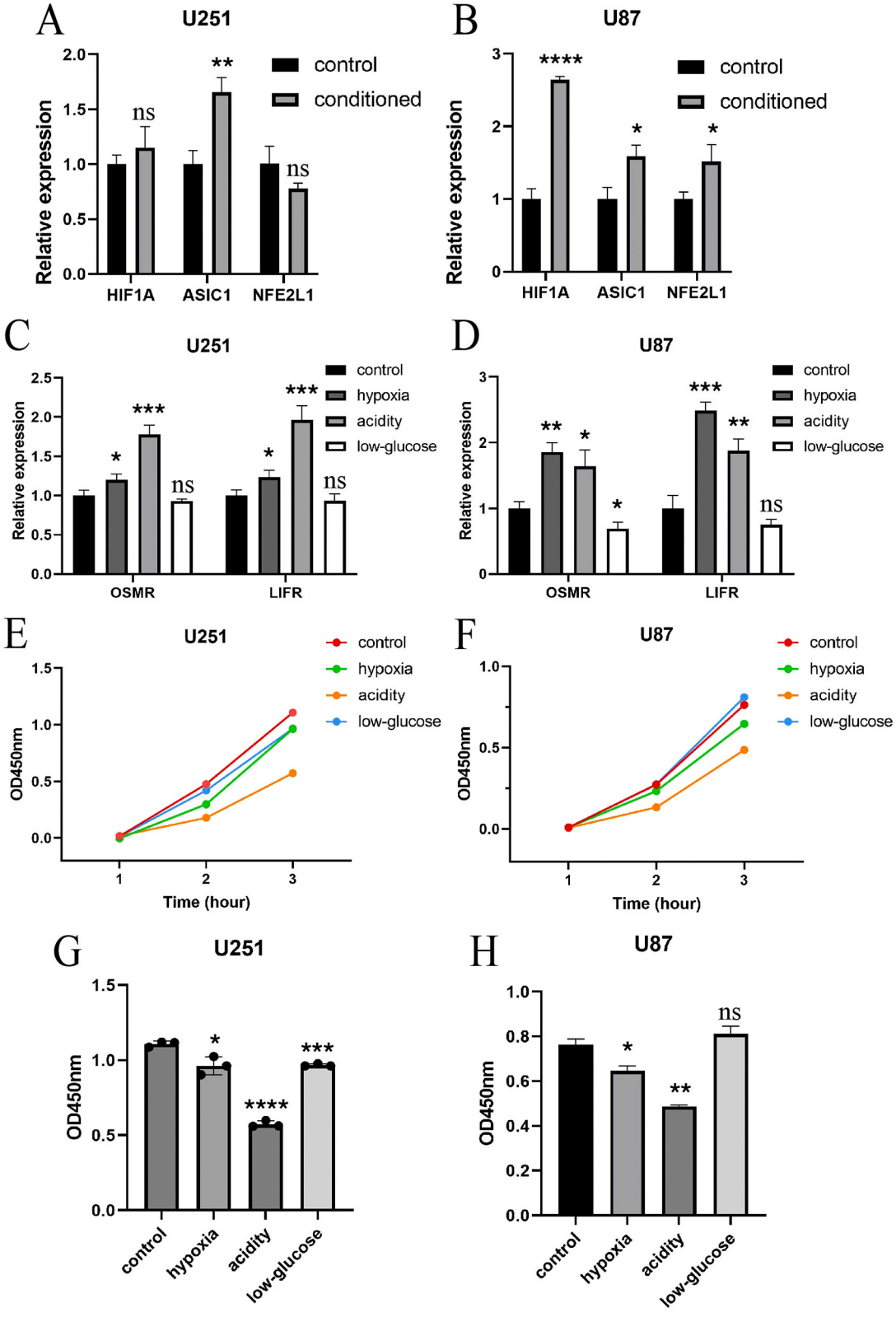

(caption on next page)

Fig. 2. | In vitro models simulated the TME stresses and revealed the relevance among TME stresses, expression of OSMR and GBM cells proliferation. **(A, B)** Sensor genes ensured the exposure to the stresses. **(C, D)** The expression of OSMR and LIFR in GBM cells under different conditions. **(E–H)** In the CCK-8 assay, acidity group displayed the highest level of proliferation inhibition among the groups. *$p < 0.05$, **$p < 0.01$, ***$p < 0.001$, ****$p < 0.0001$; ns, no significance.

hypoxia suggested that TME stress had an impact on the expression of OSMR/LIFR and further regulated the properties of GBM cells.

Three models *in vitro* were integrated to simulate TME stress in tumor core. The reliability of the models was proven by the expression of sensor genes for each TME factor. The qRT-PCR results of ASIC1 upregulation confirmed effective exposure to acidity ($p < 0.005$) (Fig. 2A and B). The differential expression of HIF1A and NFE2L1 implied that U251 and U87 cell lines might have different tolerances to hypoxic and low-glucose conditions.

This tolerance also affects OSMR expression. In U251 cells, OSMR was upregulated in the acidic and low-glucose groups, while no significant difference was observed in the hypoxic group; OSMR expression was elevated in the hypoxia and acidic groups, with no significant difference in the low-glucose group, in U87 cells (Fig. 2C and D). The expression pattern of LIFR, which participates in the suppression of invasion/metastasis in GBM cells, closely resembled that of OSMR.

Several functional experiments were performed to investigate the effects of environmental stress on the GBM properties. The CCK-8 assay revealed the varying effects of the three environmental stresses on GBM proliferation. The acidic group displayed the highest level of proliferation inhibition ($p < 0.0001$) among the groups. The hypoxic group showed slight inhibition compared to the control group ($p < 0.05$). The low-glucose condition only inhibited U251 cells (Fig. 2E–H).

Wound healing and Transwell assays provided evidence for the regulatory effects of different TME conditions on the migration and invasiveness of GBM cells. Acidic conditions enhance the invasive and migratory capabilities of both cell types. Like the expression of OSMR, hypoxia had a limited effect on the invasion and migration capabilities of U251 cells, whereas the regulatory effect of low-glucose conditions was evident. U87 cells exhibited tolerance to low-glucose conditions but were sensitive to hypoxia (Fig. 3A–D). Together, these assays revealed the varied effects of the three TME stresses on GBM cell properties.

4. Discussion

Recently, OSMR has been shown to be involved in the regulation of GBM invasiveness. In TCGA database analysis, the expression of OSMR and LIFR in the mesenchymal subtype, which exhibited high levels of necrosis and stress, indicated that environmental stresses upregulated OSMR and inhibited LIFR expression. The results of scRNA-seq analysis showed the upregulation of OSMR in core vs. peripheral tissues, while the expression of LIFR showed the opposite trend. These results imply higher invasiveness of core GBM cells [2]. The slight difference in the ligands (OSM and LIF) indicated the limited role of macrophages/microglia in OSMR/LIFR-related alterations in invasiveness.

Based on these results, the following hypothesis was proposed: Environmental stresses in the core TME, especially hypoxia, acidity and low-glucose, might induce higher invasive properties of GBM cells. After infiltrating the region conducive to cell survival, the invasive GBM cells transformed from an invasive into a proliferative phenotype. This shift caused the cells to stall in the peritumoral region and be capture in the pathological samples. Only a rare portion of the invasive GBM cells maintained their invasive properties and migrated distantly, which resulted in their inability to be captured. This hypothesis is based on the regulatory effects of TME on tumor cells.

TME is increasingly recognized as a decisive factor in GBM progression and metastasis [2]. “Go or grow” mechanism and previous studies suggested the existence of phenotypic shift and “invasive” GBM cells with high invasive and low proliferative properties [4]. To investigate the gene expression profiles of invasive and proliferative GBM cells, scRNA-seq analysis of GEO was performed using the standard Seurat package and cluster annotation. The GSEA results effectively detected the inter-regional characteristics of GBM and indicated the influence of the TME.

Microglia, which are resident macrophage in central nervous system (CNS), show similarities in classification and function [35]. They are the most important immune cell in CNS. Microglia/macrophages can polarize into M1 or M2 phenotypes, which are distinguished by their pro- or anti-inflammatory properties. In the TME of GBM, microglia/macrophages interact bidirectionally with tumor cells and exhibit a series of unique features. These cells are known as tumor-associated microglia/macrophages. The scRNA-seq analysis in this study found that TAMs in core area were more likely to be of the M2 (tumor-promoting) subtype, according to phenotypic marker genes. Intercellular communication analysis revealed the interaction between GBM cells and TAMs, and the pathways involved in both cell types, verifying the role of TAMs in GBM progression.

In vitro assays were performed to investigate the effects of microenvironmental stress on GBM cells. U251 and U87 cells exhibit differences in morphology and growth characteristics, as well as varying levels of tolerance and sensitivity to TME factors. In the acidic group, the results for both cell lines were similar, with acidity having the greatest effect on GBM proliferation, migration, and invasion. In this study, a hypoxic microenvironment was induced using $CoCl_2$, a widely used method, to accumulate HIF1a protein and subsequently regulate the expression of hypoxia-related genes. Low-glucose conditions were established using both high- and low-glucose culture media. Although the experimental methods could be further improved, such as using low-oxygen cell culture chambers and more diverse concentration gradients of glucose, the models in this study revealed differing sensitivities or tolerances of U87 and U251 cell lines to hypoxia and low-glucose conditions. In both cell lines, the expression of OSMR positively correlated with changes in the migration and invasion of GBM cells, demonstrating the reliability of OSMR as a marker gene for the invasiveness of GBM cells. LIFR expression was similar to that of OSMR, which diminishes the reliability of LIFR as a biomarker. Future research should explore and

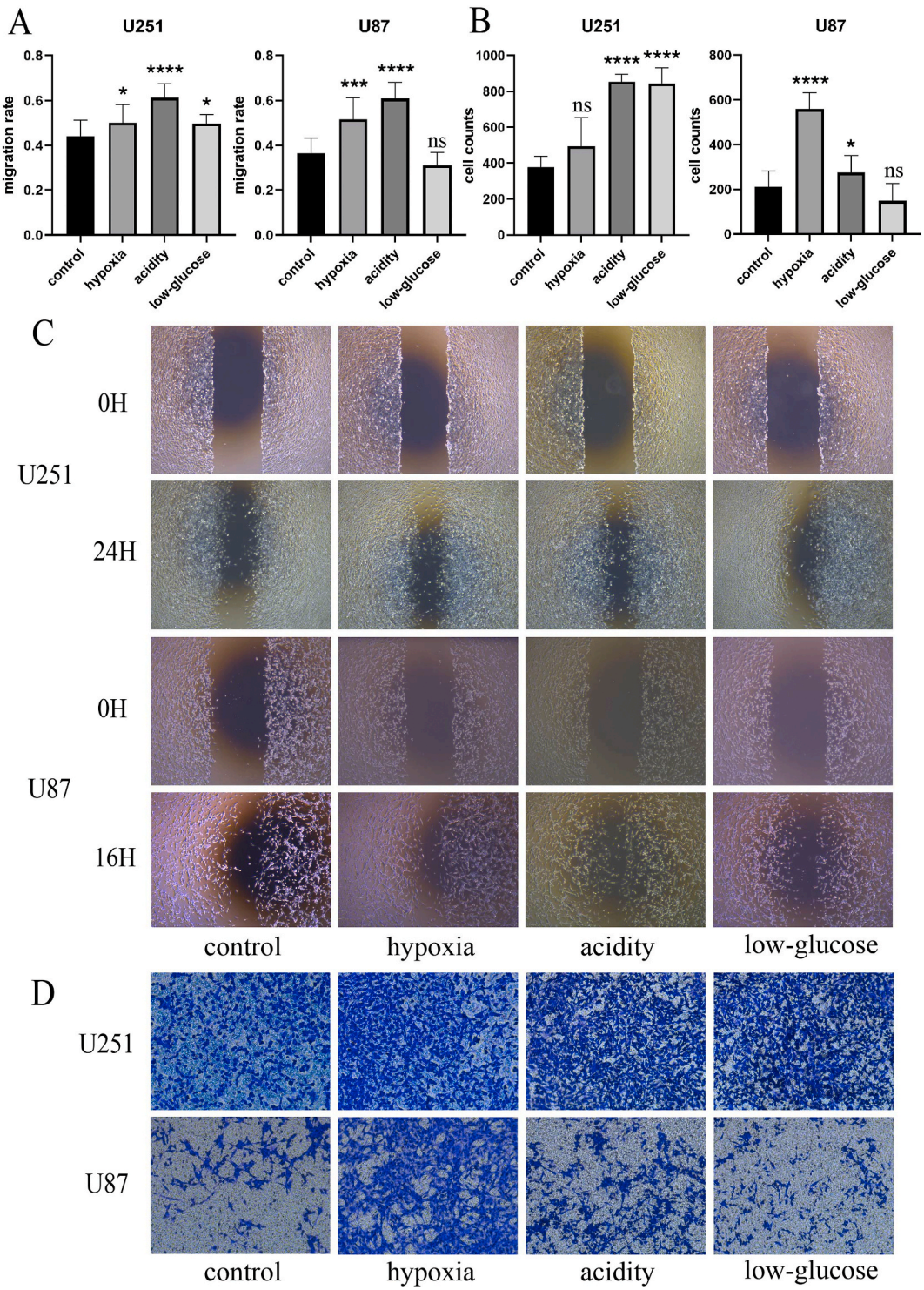

Fig. 3. | The migrative and invasive properties of GBM cells under differential stresses. **(A, C)** The wound-healing assay compared the effects of stresses on cell migration. **(B, D)** In the Transwell invasion assay, environmental stresses promoted the invasion of GBM cells at different levels. *p < 0.05, ***p < 0.001, ****p < 0.0001; ns, no significance.

discuss markers of GBM invasiveness. Overall, this study revealed a preliminary correlation among TME stress, OSMR expression, and GBM cell invasiveness.

For further verification, patient-derived orthotopic xenograft (PDX) models would be more convincing for simulating the real state

of the disease. Spatial transcriptomics of frozen sections obtained from PDX models or patients is worth investigating. Moreover, the feasibility of intervening in tumor progression by regulating TME or OSMR expression will be the focus of future research. The development of small-molecule drugs as OSMR inhibitors and TME regulators is a promising approach for GBM postoperative adjuvant therapy [36].

5. Conclusion

In this study, scRNA-seq analysis revealed the core/peripheral TMEs heterogeneity. OSMR, a marker of GBM invasion, indicated a higher invasiveness of core GBM cells. Models *in vitro* verified the relevance of TME stress, OSMR expression and GBM cell invasiveness. Thus, OSMR inhibition and TME regulation may provide new perspectives in GBM treatment.

Ethics approval and consent to participate

Not applicable.

Consent for publication

Not applicable.

Data availability

The scRNA-seq data (accession number GSE84465) was obtained from Gene Expression Omnibus (GEO, http://www.ncbi.nlm.nih.gov/geo/) database. R code used in this study was uploaded to GitHub (https://github.com/Jianyu-Zhang93/public—code-for-TME.git). Further inquiries can be directed to the corresponding authors.

Funding

This study was supported by the Health Commission of Yunnan Province, Renowned Doctors Special Program, Yunnan High-level Talents Training Support Program (grant number: KYRLMY20200026); Yunnan Applied Basic Research Project of Diagnosis and Treatment Center for Nervous System Diseases (grant number: ZX2019-03-05); Health Commission of Yunnan Province, Science and Technology Talents and Platform Program (grant number: 202105AC160029); The project for the Training of Technological Innovation Talents in Yunnan Province (grant number: 202205AD160006).

CRediT authorship contribution statement

Jianyu Zhang: Writing – review & editing, Writing – original draft, Visualization, Validation, Software, Project administration, Methodology, Investigation, Conceptualization. **Jinghui Li:** Writing – original draft, Validation, Resources, Funding acquisition, Conceptualization. **Renli Qi:** Validation, Supervision, Resources, Methodology, Investigation. **Shipeng Li:** Visualization, Validation, Methodology, Data curation. **Xin Geng:** Visualization, Validation, Software, Funding acquisition. **Hong Shi:** Writing – review & editing, Supervision, Resources, Funding acquisition, Conceptualization. **Hualin Yu:** Writing – review & editing, Writing – original draft, Supervision, Project administration, Funding acquisition, Conceptualization.

Declaration of competing interest

The authors declare that they have no known competing financial interests or personal relationships that could have appeared to influence the work reported in this paper.

Acknowledgments

We thank Prof. Xuebin Qi and Hui Zhang for support and advice, thank all members in our study group for the help and advice.

Appendix A. Supplementary data

Supplementary data to this article can be found online at https://doi.org/10.1016/j.heliyon.2024.e35770.

References

[1] W. Michael, W. Wolfgang, A. Ken, B. Michael, B. Mitchell, P.S. M, N. Ryo, R. Mark, W.P. Y, S. Roger, et al., Glioma, Nat. Rev. Dis. Prim. 1 (2015).

[2] C.A. Liu, C.Y. Chang, K.W. Hsueh, H.L. Su, T.W. Chiou, S.Z. Lin, H.J. Harn, Migration/invasion of malignant gliomas and implications for therapeutic treatment, Int. J. Mol. Sci. 19 (2018), https://doi.org/10.3390/ijms19041115.

[3] A.M. Reuss, D. Groos, M. Buchfelder, N. Savaskan, The acidic brain-glycolytic switch in the microenvironment of malignant glioma, Int. J. Mol. Sci. 22 (2021), https://doi.org/10.3390/ijms22115518.

[4] H. Hatzikirou, D. Basanta, M. Simon, K. Schaller, A. Deutsch, 'Go or grow': the key to the emergence of invasion in tumour progression? Math. Med. Biol. 29 (2012) 49–65, https://doi.org/10.1093/imammb/dqq011.

[5] A. Franson, B.L. McClellan, M.L. Varela, A. Comba, M.F. Syed, K. Banerjee, Z. Zhu, N. Gonzalez, M. Candolfi, P. Lowenstein, et al., Development of immunotherapy for high-grade gliomas: overcoming the immunosuppressive tumor microenvironment, Front. Med. 9 (2022) 966458, https://doi.org/10.3389/fmed.2022.966458.

[6] N.A. Charles, E.C. Holland, R. Gilbertson, R. Glass, H. Kettenmann, The Brain Tumor Microenvironment, vol. 59, John Wiley & Sons, Ltd, 2011.

[7] M. Qianquan, L. Wenyong, X. Changsheng, C. Junjun, L. Mei, W.H. Y, L. Qing, W. Rong-Fu, Cancer stem cells and immunosuppressive microenvironment in glioma, Front. Immunol. 9 (2018).

[8] C. Andrea, G. Irene, C. Sabrina, G. Caroline, M. Aristidis, S. Patricia, C. Laia, Glucose and amino acid metabolic dependencies linked to stemness and metastasis in different aggressive cancer types, Front. Pharmacol. 12 (2021).

[9] H. Elisabeth, H.P. Nikolaus, S. Janina, S. Jens, B. Hans-Jörg, B. Shohag, v.H. Elke, Z. Cornelia, M. Michel, N. Ulrike, The "go or grow" potential of gliomas is linked to the neuropeptide processing enzyme carboxypeptidase E and mediated by metabolic stress, Acta Neuropathol. 124 (2012).

[10] R.G. Verhaak, K.A. Hoadley, E. Purdom, V. Wang, Y. Qi, M.D. Wilkerson, C.R. Miller, L. Ding, T. Golub, J.P. Mesirov, et al., Integrated genomic analysis identifies clinically relevant subtypes of glioblastoma characterized by abnormalities in PDGFRA, IDH1, EGFR, and NF1, Cancer Cell 17 (2010) 98–110, https://doi.org/10.1016/j.ccr.2009.12.020.

[11] S. Darmanis, S.A. Sloan, D. Croote, M. Mignardi, S. Chernikova, P. Samghababi, Y. Zhang, N. Neff, M. Kowarsky, C. Caneda, et al., Single-cell RNA-seq analysis of infiltrating neoplastic cells at the migrating front of human glioblastoma, Cell Rep. 21 (2017).

[12] X.G. Zihao Wang, Bing Xing, Glioblastoma cell differentiation trajectory predicts the immunotherapy response and overall survival of patients, Aging 12 (2020).

[13] K. Yu, Y. Hu, F. Wu, Q. Guo, Z. Qian, W. Hu, J. Chen, K. Wang, X. Fan, X. Wu, et al., Surveying brain tumor heterogeneity by single-cell RNA-sequencing of multi-sector biopsies, Natl. Sci. Rev. 7 (2020) 1306–1318.

[14] F. Lantieri, T. Bachetti, OSM/OSMR and interleukin 6 family cytokines in physiological and pathological condition, Int. J. Mol. Sci. 23 (2022), https://doi.org/10.3390/ijms231911096.

[15] K. A, R. K, K. W, S. R, B. T, D. J, T. J, K. A, B. M, K. T, Differential effects of oncostatin M and leukaemia inhibitory factor expression in astrocytoma cells, Biochem. J. (2001) 355.

[16] P.C. Heinrich, I. Behrmann, S. Haan, H.M. Hermanns, G. Müller-Newen, F. Schaper, Principles of interleukin (IL)-6-type cytokine signalling and its regulation, Biochem. J. 374 (2003) 1–20, https://doi.org/10.1042/bj20030407.

[17] K. Natesh, D. Bhosale, A. Desai, G. Chandrika, R. Pujari, J. Jagtap, A. Chugh, D. Ranade, P. Shastry, Oncostatin-M differentially regulates mesenchymal and proneural signature genes in gliomas via STAT3 signaling, Neoplasia 17 (2015) 225–237, https://doi.org/10.1016/j.neo.2015.01.001.

[18] C. Joe, O.J. Thom, L. J.C, Emerging perspectives on leukemia inhibitory factor and its receptor in cancer, Front. Oncol. 11 (2021).

[19] T. Stuart, A. Butler, P. Hoffman, C. Hafemeister, E. Papalexi, W.M. Mauck, Y. Hao, M. Stoeckius, P. Smibert, R. Satija, Comprehensive integration of single-cell data, Cell 177 (2019), https://doi.org/10.1016/j.cell.2019.05.031, 1888-1902.e1821.

[20] X. Shao, J. Liao, X. Lu, R. Xue, N. Ai, X. Fan, scCATCH: automatic annotation on cell types of clusters from single-cell RNA sequencing data, iScience 23 (2020) 100882, https://doi.org/10.1016/j.isci.2020.100882.

[21] D. Aran, A.P. Looney, L. Liu, E. Wu, V. Fong, A. Hsu, S. Chak, R.P. Naikawadi, P.J. Wolters, A.R. Abate, et al., Reference-based analysis of lung single-cell sequencing reveals a transitional profibrotic macrophage, Nat. Immunol. 20 (2019) 163–172, https://doi.org/10.1038/s41590-018-0276-y.

[22] T. Mou, W. Deng, F. Gu, Y. Pawitan, T.N. Vu, Reproducibility of methods to detect differentially expressed genes from single-cell RNA sequencing, Front. Genet. 10 (2019) 1331, https://doi.org/10.3389/fgene.2019.01331.

[23] A. Subramanian, P. Tamayo, V.K. Mootha, S. Mukherjee, B.L. Ebert, M.A. Gillette, A. Paulovich, S.L. Pomeroy, T.R. Golub, E.S. Lander, et al., Gene set enrichment analysis: a knowledge-based approach for interpreting genome-wide expression profiles, Proc. Natl. Acad. Sci. U. S. A. 102 (2005) 15545–15550, https://doi.org/10.1073/pnas.0506580102.

[24] S. Jin, C.F. Guerrero-Juarez, L. Zhang, I. Chang, R. Ramos, C.H. Kuan, P. Myung, M.V. Plikus, Q. Nie, Inference and analysis of cell-cell communication using CellChat, Nat. Commun. 12 (2021) 1088, https://doi.org/10.1038/s41467-021-21246-9.

[25] M. Efremova, M. Vento-Tormo, S.A. Teichmann, R. Vento-Tormo, CellPhoneDB: inferring cell-cell communication from combined expression of multi-subunit ligand-receptor complexes, Nat. Protoc. 15 (2020) 1484–1506, https://doi.org/10.1038/s41596-020-0292-x.

[26] Z. Tang, B. Kang, C. Li, T. Chen, Z. Zhang, GEPIA2: an enhanced web server for large-scale expression profiling and interactive analysis, Nucleic Acids Res. 47 (2019) W556–w560, https://doi.org/10.1093/nar/gkz430.

[27] K. Duan, Z.J. Liu, S.Q. Hu, H.Y. Huo, Z.R. Xu, J.F. Ruan, Y. Sun, L.P. Dai, C.B. Yan, W. Xiong, et al., Lactic acid induces lactate transport and glycolysis/OXPHOS interconversion in glioblastoma, Biochem. Biophys. Res. Commun. 503 (2018) 888–894, https://doi.org/10.1016/j.bbrc.2018.06.092.

[28] S.C. Nunes, F. Lopes-Coelho, S. Gouveia-Fernandes, C. Ramos, S.A. Pereira, J. Serpa, Cysteine boosters the evolutionary adaptation to CoCl(2) mimicked hypoxia conditions, favouring carboplatin resistance in ovarian cancer, BMC Evol. Biol. 18 (2018) 97, https://doi.org/10.1186/s12862-018-1214-1.

[29] S. Zhu, H.Y. Zhou, S.C. Deng, S.J. Deng, C. He, X. Li, J.Y. Chen, Y. Jin, Z.L. Hu, F. Wang, et al., ASIC1 and ASIC3 contribute to acidity-induced EMT of pancreatic cancer through activating Ca(2+)/RhoA pathway, Cell Death Dis. 8 (2017) e2806, https://doi.org/10.1038/cddis.2017.189.

[30] V.K. Tripathi, S.A. Subramaniyan, I. Hwang, Molecular and cellular response of Co-cultured cells toward cobalt chloride (CoCl(2))-induced hypoxia, ACS Omega 4 (2019) 20882–20893, https://doi.org/10.1021/acsomega.9b01474.

[31] B. Keith, M.C. Simon, Hypoxia-inducible factors, stem cells, and cancer, Cell 129 (2007) 465–472, https://doi.org/10.1016/j.cell.2007.04.019.

[32] C. Jin, Q.H. Ye, F.L. Yuan, Y.L. Gu, J.P. Li, Y.H. Shi, X.M. Shen, L. Bo, Z.H. Lin, Involvement of acid-sensing ion channel 1α in hepatic carcinoma cell migration and invasion, Tumour Biol 36 (2015) 4309–4317, https://doi.org/10.1007/s13277-015-3070-6.

[33] L. Qiu, Q. Yang, W. Zhao, Y. Xing, P. Li, X. Zhou, H. Ning, R. Shi, S. Gou, Y. Chen, et al., Dysfunction of the energy sensor NFE2L1 triggers uncontrollable AMPK signaling and glucose metabolism reprogramming, Cell Death Dis. 13 (2022) 501, https://doi.org/10.1038/s41419-022-04917-3.

[34] W.N. R, M.J. I, W.P. H, Oncostatin-M promotes phenotypic changes associated with mesenchymal and stem cell-like differentiation in breast cancer, Oncogene 33 (2014).

[35] U.K. Hanisch, H. Kettenmann, Microglia: active sensor and versatile effector cells in the normal and pathologic brain, Nat. Neurosci. 10 (2007) 1387–1394, https://doi.org/10.1038/nn1997.

[36] S. Viswanadhapalli, Y. Luo, G.R. Sareddy, B. Santhamma, M. Zhou, M. Li, S. Ma, R. Sonavane, U.P. Pratap, K.A. Altwegg, et al., EC359: a first-in-class small-molecule inhibitor for targeting oncogenic LIFR signaling in triple-negative breast cancer, Mol. Cancer Therapeut. 18 (2019) 1341–1354, https://doi.org/10.1158/1535-7163.Mct-18-1258.